



Myelin water imaging of moderate to severe diffuse traumatic brain injury

Joon Yul Choi^{a,2}, Tessa Hart^b, John Whyte^b, Amanda R. Rabinowitz^b, Se-Hong Oh^c,
Jongho Lee^{a,*,1}, Junghoon J. Kim^{d,*,1}

^a Laboratory for Imaging Science and Technology, Department of Electrical and Computer Engineering, Institute of Engineering Research, Seoul National University, 1 Gwanak-ro, Gwanak-gu, Seoul 08826, Republic of Korea

^b Moss Rehabilitation Research Institute, 50 Township Line Road, Elkins Park, PA 19027, USA

^c Department of Biomedical Engineering, Hankuk University of Foreign Studies, 81, Oedae-ro, Mohyeon-myeon, Cheoin-gu, Yongin-si, Gyeonggi-do, 17035, Republic of Korea

^d Department of Molecular, Cellular, and Biomedical Sciences, CUNY School of Medicine, The City College of New York, 160 Convent Avenue, New York, NY 10031, USA

ARTICLE INFO

Keywords:

Traumatic brain injury
Myelin water imaging
Diffusion tensor imaging
Processing speed index
Post traumatic amnesia

ABSTRACT

Traumatic axonal injury (TAI), a signature injury of traumatic brain injury (TBI), is increasingly known to involve myelin damage. The objective of this study was to demonstrate the clinical relevance of myelin water imaging (MWI) by first quantifying changes in myelin water after TAI and then correlating those changes with measures of injury severity and neurocognitive performance. Scanning was performed at 3 months post-injury in 22 adults with moderate to severe diffuse TBI and 30 demographically matched healthy controls using direct visualization of short transverse component (ViSta) MWI. Fractional anisotropy (FA) and radial diffusivity (RD) were also obtained using diffusion tensor imaging. Duration of post-traumatic amnesia (PTA) and cognitive processing speed measured by the Processing Speed Index (PSI) from Wechsler Adult Intelligence Scale-IV, were assessed. A between-group comparison using Tract-Based Spatial Statistics revealed that there was a widespread reduction of apparent myelin water fraction (aMWF) in TBI, consistent with neuropathology involving TAI. The group difference map of aMWF yielded topography that was different from FA and RD. Importantly, aMWF demonstrated significant associations with PTA ($r = -0.564$, $p = .006$) and PSI ($r = 0.452$, $p = .035$). In conclusion, reduced myelin water, quantified by ViSta MWI, is prevalent in moderate-to-severe diffuse TBI and could serve as a potential biomarker for injury severity and prediction of clinical outcomes.

1. Introduction

Traumatic brain injury (TBI) is one of the leading causes of mortality and morbidity worldwide (Maas et al., 2008). Traumatic axonal injury (TAI), or diffuse axonal injury (DAI), is a hallmark of TBI and is more predictive of behavioral outcome than focal injury in case of moderate to severe TBI (Katz and Alexander, 1994; Ross et al., 1994). Because accurate assessment of the extent of TAI is not currently feasible using conventional T₁- and T₂-weighted images, diffusion tensor

imaging (DTI) has been widely used to evaluate white matter (WM) damage after TBI (Kraus et al., 2007; Newcombe et al., 2007). This has represented an important advance in characterizing WM changes associated with TBI. However, DTI is inherently limited in distinguishing among white matter pathologies such as damage to axonal membranes, myelin sheath, or other components of the microstructure (Jurick et al., 2016; Liu et al., 2011; Shenton et al., 2012).

Myelin has increasingly been considered an important component in the pathophysiology of TBI. Histological studies have demonstrated

Abbreviations: aMWF, apparent myelin water fraction; DAI, diffuse axonal injury; FA, fractional anisotropy; GE, gradient echo; HC, healthy control; MWI, myelin water imaging; PD, proton density; PSI, processing speed index; PTA, post-traumatic amnesia; RD, radial diffusivity; TAI, traumatic axonal injury; TBI, traumatic brain injury; TBSS, tract-based spatial statistics; ViSta, direct visualization of short transverse relaxation time component; WM, white matter

* Corresponding author at: Department of Molecular, Cellular, and Biomedical Sciences, CUNY School of Medicine, The City College of New York, Harris Hall, 160 Convent Avenue, New York, NY, USA.

** Corresponding author at: Laboratory for Imaging Science and Technology, Department of Electrical and Computer Engineering, Institute of Engineering Research, Seoul National University, Building 301, Room 1008, 1 Gwanak-ro, Gwanak-gu, Seoul, Republic of Korea.

E-mail addresses: thart@einstein.edu (T. Hart), jwhyte@einstein.edu (J. Whyte), RabinowA@einstein.edu (A.R. Rabinowitz), jonghoyi@snu.ac.kr (J. Lee), jkim@med.cuny.edu (J.J. Kim).

¹ Jongho Lee and Junghoon Kim are co-corresponding authors.

² The current affiliation of the first author is Epilepsy Center, Neurological Institute, Cleveland Clinic, OH 44106, USA.

<https://doi.org/10.1016/j.nicl.2019.101785>

Received 22 July 2018; Received in revised form 8 March 2019; Accepted 16 March 2019

Available online 16 March 2019

2213-1582/ © 2019 The Authors. Published by Elsevier Inc. This is an open access article under the CC BY-NC-ND license (<http://creativecommons.org/licenses/by-nc-nd/4.0/>).

that TBI induces widespread myelin loss in the rodent and the ex-vivo human brain. Experimentally injured mice have shown significant myelin loss from 3 days to 6 weeks post-TBI compared to mice that have undergone sham surgery using electron microscopy (Mierzwa et al., 2015). Additionally, chronic myelin loss is also observed in the rodents with experimental TBI (Bramlett and Dietrich, 2002). Histochemical analysis of DAI in post-mortem human brains has also revealed acute myelin loss in WM (Ng et al., 1994). Accumulating evidence suggests that the myelin loss in TBI may affect neuronal signaling and cognitive function (Kinnunen et al., 2011; Sharp et al., 2011). Thus, myelin may be an important target for TBI diagnosis, prognosis, and intervention.

In this study, we investigated changes in myelin water in moderate to severe TBI using a new myelin water imaging (MWI) method, direct visualization of short transverse relaxation time component (ViSTa). The ViSTa sequence utilizes double inversion preparation pulses to suppress long T_1 components. The remaining signal is a short T_2^* signal from myelin water (Oh et al., 2013). The ViSTa signal has been validated as a measure of myelin water by T_2^* characteristics (Oh et al., 2013), phase evolution (Kim et al., 2015), and magnetization transfer effects (Lee et al., 2014). ViSTa has improved image quality and reproducibility compared to the conventional MWI used in prior works (Oh et al., 2013; Oh et al., 2014). For the quantitative analysis, ViSTa myelin water fraction (MWF) was calculated by dividing ViSTa data by proton density (PD) weighted gradient echo (GE) data and multiplying it by a scaling factor (Oh et al., 2013). The resulting ViSTa MWF was referred to as the apparent MWF (aMWF), which was roughly one third of conventional MWF due to the incomplete scaling factor (Choi et al., 2018). In clinical application, ViSTa MWI has been used for evaluation of demyelination in multiple sclerosis (Choi et al., 2016) and neuro-myelitis optica disorder syndrome (Jeong et al., 2017).

Recently, the first human in vivo study using T2-relaxation based MWI demonstrated a reduction in MWF at 2 weeks post-injury in mild TBI patients (Wright et al., 2016). However, to be established as a clinically relevant biomarker of myelin damage, reduction in myelin water should be related to injury severity and neurocognitive performance. The main purpose of the present study was to examine the clinical relevance of aMWF by assessing its relationship to measures of overall severity of TAI and post-traumatic impairment in cognitive processing speed in patients who sustained moderate to severe diffuse TBI. In this study, post-traumatic amnesia (PTA) duration was selected as the severity measure rather than Glasgow Coma Scale because PTA has been shown to be a superior predictor of TBI outcome in head-to-head comparisons (Ponsford, 2013). Standard DTI metrics were also acquired and analyzed reference purposes. However, a direct map-wise comparison of aMWF and DTI metrics was not conducted due to the inherent differences between the two image types in terms of spatial resolution and signal distribution.

2. Material and methods

2.1. Study participants

Thirty-one adults with moderate to severe TBI were initially enrolled from a specialized inpatient rehabilitation unit. Inclusion criteria were: age between 18 and 64 years old and a diagnosis of non-penetrating moderate to severe TBI as defined by at least one of the following: (1) Glasgow Coma Scale score < 13 in Emergency Department (not due to sedation, paralysis or intoxication); (2) loss of consciousness ≥ 12 h; (3) prospectively documented PTA ≥ 24 h. To ensure that the TBI was predominantly diffuse, participants were required to have experienced a high-velocity, high-impact injury mechanism resulting in immediate loss of consciousness.

Participants were excluded for: 1) history of prior TBI, CNS disease, seizure disorder, schizophrenia, or bipolar disorder, 2) history of serious alcohol or psychostimulant (e.g., cocaine) abuse because it could have had deleterious neurologic effects, 3) pregnancy, 4) inability to

Table 1

Demographic and clinical characteristics of the study cohort.

	TBI (N = 22)	HC (N = 30)	Effect size	p value
Age (y) [†]	31.5 \pm 13.4	36.5 \pm 10.0	0.490	0.135
Gender (male: female) [‡]	16: 6	23: 7	–	0.746
Education (y) [†]	14.0 \pm 2.3	13.1 \pm 2.2	0.409	0.170
Days post-injury	105.7 \pm 21.0	–	–	–
Focal lesion volume (cm ³)	7.7 \pm 10.1	–	–	–
Post-traumatic amnesia (day) [§]	26.0 (1–76)	–	–	–
Processing speed index [§]	90.8 (53–132)	–	–	–
Mechanism of injury				
Vehicular	82%	–	–	–
Falls	18%	–	–	–

2 cases were discharged from rehabilitation while still in post-traumatic amnesia. The values for age, education, days post-injury, and focal lesion volume indicate mean \pm standard deviation. Effect sizes are Cohen's d.

[†] p values from Student *t*-tests.

[‡] p values from Chi-square test.

[§] Mean value (range), N = 20.

undergo MRI scanning due to ferromagnetic implants, claustrophobia, or restlessness, 5) non-fluency in English, 6) level of impairment precluding the subject's ability to complete testing and scanning at 3-months post-TBI, or 7) large focal intraparenchymal lesions on acute CT or MRI (approximately > 5 cm³ for subcortical lesions and 50 cm³ for cortical lesions estimated by visual inspection).

Thirty-five healthy controls (HC) comparable to TBI subjects in age, gender, and years of education were recruited. Exclusion criteria for HC were the same as above, with the addition of exclusion for any history of TBI resulting in alteration or loss of consciousness. The study was approved by the Institutional Review Board of the home institution and all participants provided written informed consent prior to the participation. Five control and nine patient participants were excluded after data quality assurance procedures, due to low MR image quality from excessive motion and/or flow artifacts during scanning ($n = 9$), and registration failure to a template image for post-processing ($n = 5$). As a result, the final analysis included data from 22 TBI and 30 HC. The demographics of these subjects are summarized in Table 1. To confirm that there was no significant group difference, Student's *t*-test was used for age and years of education and Chi-square test was used for gender. The two groups did not differ in age, gender, and years of education. More precise quantification of focal encephalomalacia after the first MRI scanning session affirmed that our rule of thumb (i.e., cortical 50 and subcortical 5 cm³ by visual inspection) of screening worked well. In fact, out of 22 patients, 7 patients did not show any visible focal lesion and only three patients had total lesion volume larger than 20 cm³.

2.2. MRI data acquisition

Participants with TBI were scanned using 3 T MRI (Trio, Siemens, Erlangen, Germany) with an 8-channel phased array head coil.

For ViSTa MWI, a 3D segmented EPI-based ViSTa sequence (Oh et al., 2013) was implemented using the following parameters: repetition time (TR) = 1160 ms; echo time (TE) = 4.5 ms; the duration between the first and second inversion (TI₁) = 560 ms; the duration between the second inversion and the excitation (TI₂) = 220 ms; the duration from the excitation and the first inversion (TD) = 380 ms; matrix size = 160 \times 160; in-plane resolution = 1.4 \times 1.4 \times 5.0 mm³; number of slices = 26; partial k-space = 6/8 in z-direction, EPI factor = 15; bandwidth = 1008 Hz/px; scan time = 7 min 33 s. Fat and flow saturation pulses were applied to prevent artifacts from those. To quantify MWF, a PD-weighted GE sequence based on the same EPI as the ViSTa sequence, but without the two inversion pulses, was acquired (TR = 97 ms; flip angle = 28°; scan time = 38 s).

A 2D EPI based DTI sequence was acquired (direction = 30; b-

values = 0 s/mm^2 ($n = 5$) and 1000 s/mm^2 ; TR = 6500 ms; TE = 84 ms; flip angle = 90° ; matrix size = 112×112 ; in plane resolution = $2.2 \times 2.2 \times 2.2 \text{ mm}^3$; number of slices = 57; GRAPPA acceleration factor = 3; bandwidth = 1860 Hz/px; scan time = 4 min). To improve signal to noise ratio, DTI was acquired two times and averaged. In addition to MWI and DTI sequences, a routine structural whole brain 3D T_1 -weighted magnetization-prepared rapid gradient echo (MPRAGE) was acquired.

2.3. Data processing

For the quantitative analysis, the ViSta aMWF was calculated by dividing the acquired ViSta data by the PD weighted GE data with 28° flip angle and multiplying by a scaling factor. This was employed to compensate for TR and flip angle differences between GE and ViSta and for T_2^* decays in GE and ViSta using nominal values (T_1 of GE signal = 800 ms, T_2^* of GRE signal = 40 ms, T_2^* of ViSta signal = 10 ms), as suggested in the literature (Oh et al., 2013). From the DTI data, fractional anisotropy (FA) and radial diffusivity (RD) were computed using DTIFIT in FSL.

To investigate statistical group differences between TBI and HC, we generated separate skeletons of aMWF and FA. Because aMWF and FA measure different quantities of the brain tissue, the skeletons of aMWF and FA were generated independently. RD used the same skeleton as FA. All images, including aMWF and FA maps, were registered non-linearly to the Johns Hopkins White Matter Atlas FA map (1mm^3 isotropic template) using SyN in Advanced Normalization Tools (ANTs) (Avants and Gee, 2004; Avants et al., 2010) after skull extraction of the images using Brain Extraction Tool (BET) in FSL (Smith, 2002). We compared registration quality of SyN, SPM, FSL, and AFNI prior to the following data processing and then chose SyN as showing the best alignment to the FA atlas map as well as the best alignment between subjects. For RD maps, we registered them non-linearly to the FA atlas map using warping matrices of FA maps generated in the previous step. Skeletons of aMWF and FA were made using FSL (Smith et al., 2006). The number of voxels within aMWF and FA skeletons were 49,856 and 64,105, respectively.

2.4. Clinical measures

Duration of PTA and cognitive processing speed were evaluated as measures of clinical outcomes.³ PTA duration, a sensitive index of the severity of neurologic injury, was calculated as the number of days between the TBI and the first of two occasions within 72 h that the participant was fully oriented. Full orientation was defined as a score above 25 on the Orientation Log (Jackson et al., 1998) or documentation of consistent orientation for 72 h in the acute medical record (i.e., prior to rehabilitation admission).

Participants were evaluated at the time of scanning with a neuropsychological battery including measures of attention, verbal learning, executive functioning, and cognitive processing speed. Processing speed was selected for this study a priori because prior work has demonstrated that processing speed measures are sensitive to TBI in general (Mathias and Wheaton, 2007) and TBI-related WM changes in particular (Felmingham et al., 2004). For the purpose of the present study, we examined the Processing Speed Index (PSI) from the Wechsler Adult Intelligence Scale IV (Wechsler and Coalson, 2008), which was

³ A common method of prospective measurement of PTA duration is to administer a standardized measure of orientation to time, place, and circumstances approximately every 3 days (72 h). Once the person has achieved correct responses twice in a row, defined by an empirically determined cutoff score on the measure of choice, the first date is used as the day emerged from PTA, while the second date establishes reliability of the measurement (since orientation can fluctuate up and down as the person is emerging).

constructed from age-corrected scores of Digit Symbol and Symbol Search subtests.

2.5. Data analysis

For the voxel-level group difference between TBI and HC, we performed Tract-Based Spatial Statistics (TBSS) analysis using the skeletons of aMWF, FA, and RD. A two-sample permutation t -test with covariates of age and gender was conducted by “randomise” in FSL on each voxel of the skeleton (Winkler et al., 2014) with Threshold-Free Cluster Enhancement (Smith and Nichols, 2009). Statistical significance was defined by the family-wise error (FWE) rate corrected p value (< 0.05). Additionally, to compare the mean global aMWF, FA, and RD values in TBI with those in HC, all voxels on the skeletons were averaged for each subject. A Mann-Whitney U test was used to evaluate the statistical difference between the groups ($p < .05$).

The relationships among three MRI metrics (aMWF, FA, and RD) were examined with Spearman's rank-order correlations. To investigate the clinical relevance of these MRI metrics, Spearman's correlation coefficients were calculated between mean global aMWF, FA, and RD and the duration of PTA and the PSI scaled score. P values $< .05$ were considered to indicate statistical significance and two-sided tests were used for all statistical analyses. All of the statistical analyses on global MRI metrics were conducted using the Statistical Package for the Social Sciences version 21.0 (SPSS Inc., Chicago, IL, USA).

3. Results

3.1. Group differences in MRI metrics

As shown in Fig. 1, voxel-wise comparisons of aMWF and FA between the two groups showed statistically significant widespread reductions in TBI patients compared to HC ($*p < .05$) while showing significantly higher RD in TBI compared to HC, demonstrating that diffuse injury causes spatially substantial damage to WM. Supplementary Fig. 1 shows un-thresholded t -maps from voxel-wise comparisons of aMWF and DTI metrics between the two groups. In widespread regions, the t -values of the DTI metrics were higher than those of aMWF.

Comparing mean global values, the aMWF values in TBI were significantly reduced relative to HC (HC = $3.4 \pm 0.3\%$, TBI = $3.2 \pm 0.4\%$, and $p = .049$) (Table 2 and Fig. 2). The mean global DTI parameters in TBI were also significantly different relative to HC ($p < .001$), with the TBI group exhibiting lower FA and higher RD. The effect sizes for group differences between TBI and HC were large for both aMWF and DTI metrics (aMWF = 0.769 (95% confidence interval (CI): 0.199, 1.339), FA = 1.727 (95% CI: 1.085, 2.370), and RD = 1.761 (95% CI: 1.115, 2.407).

3.2. Correlation among MRI metrics

To examine the relationship of aMWF with other DTI metrics, Spearman's rank-order correlations were calculated using mean global aMWF, FA, and RD values. Fig. 3 displays scatter plots showing the bivariate correlation pattern among the three MRI metrics in HC and TBI groups. While the mean global FA and RD values were highly correlated with each other in both groups ($\rho = -0.845$ for HC, $\rho = -0.957$ for TBI), these DTI metrics were not significantly correlated with aMWF in HC ($\rho = 0.002$ for FA, $\rho = -0.242$ for RD) and only moderately correlated with aMWF in TBI ($\rho = 0.468$ for FA, $\rho = -0.553$ for RD), in agreement with the previous result that DTI metrics may not reflect myelin (Liu et al., 2011). This pattern of correlation is compatible with the notions that 1) RD may be a better indicator of myelination than FA and 2) aMWF may offer complementary information to conventional DTI.

Fig. 4 shows representative T_1 weighted, aMWF, FA, and RD images of HC and TBI subjects. The intensity distributions of ViSta aMWF and

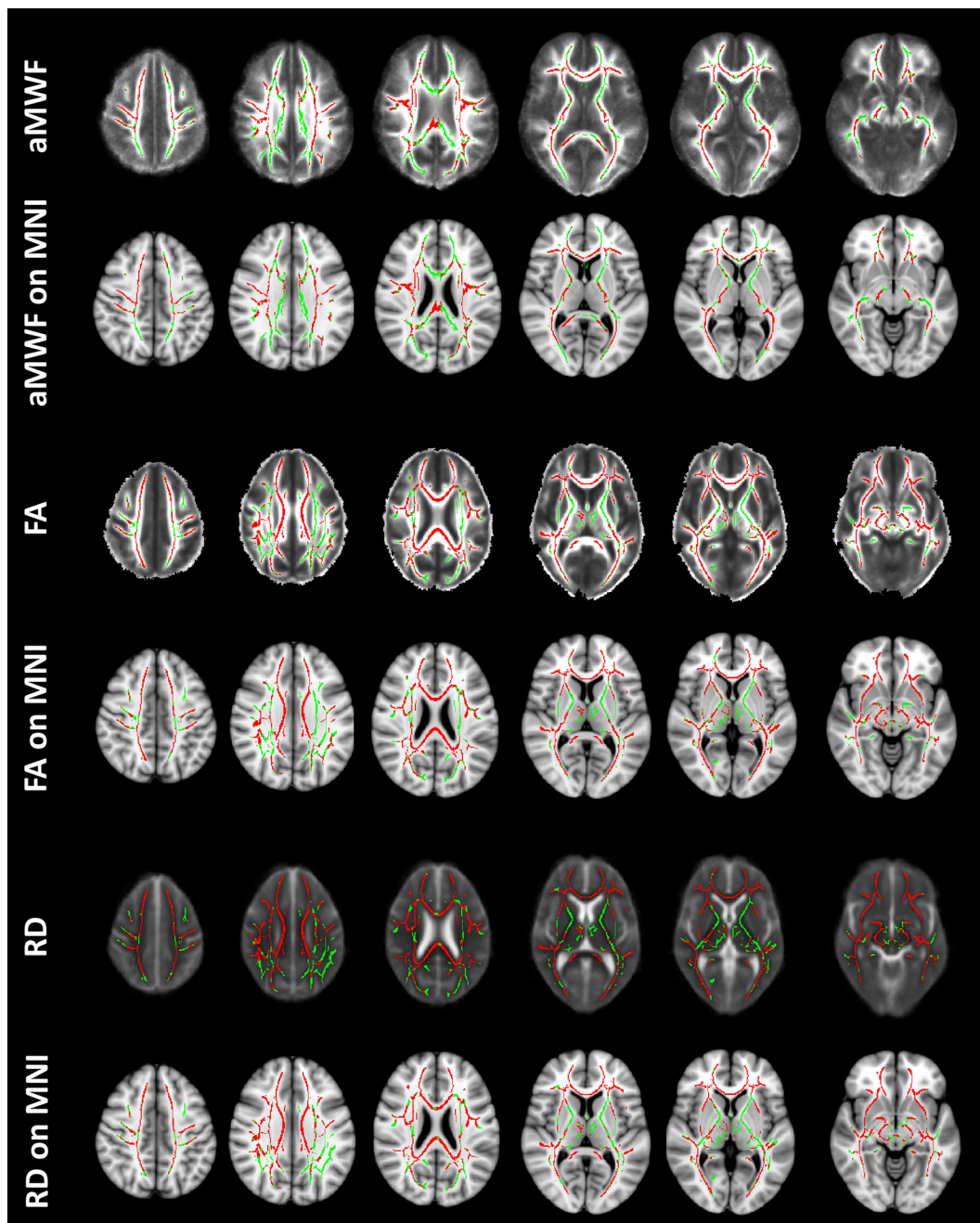


Fig. 1. Voxel-wise TBSS analysis results for comparison of whole brain aMWF (first and second rows), FA (third and fourth rows), and RD (fifth and sixth rows) between TBI patients and healthy controls. Widespread regions in the brain show lower aMWF and FA, and higher RD in TBI patients ($p < .05$, FWE-corrected). Green: skeleton, red: significant voxels. First (aMWF), third (FA), and fifth (RD) skeletons are overlaid on the group template generated for each metric. Second (aMWF), fourth (FA), and sixth (RD) skeletons are displayed on the Colin-brain atlas in MNI space. (Color figure).

Table 2
Mean global values of imaging metrics in the study cohort.

	TBI (N = 22)	HC (N = 30)	Effect size	p value
aMWF (%) [§]	3.2 ± 0.4	3.4 ± 0.3	0.769	0.049*
FA [§]	0.47 ± 0.03	0.51 ± 0.02	1.727	< 0.001**
RD [§]	0.0577 ± 0.0044	0.0532 ± 0.0025	1.761	< 0.001**

aMWF: apparent myelin water fraction, FA: fractional anisotropy, and RD: radial diffusivity. The values are mean ± standard deviation of all voxels on each global white matter skeleton. Effect sizes are Cohen's d

[§] p values from Mann-Whitney U test.

* $p < .05$.

** $p < .01$.

FA maps reveal subtle differences between the two maps. The yellow arrows in Fig. 4 point to the ‘black holes’ in conventional DTI images due to crossing fibers (Landman et al., 2010). However, aMWF shows a much smaller degree of attenuation in those areas, demonstrating MWI's insensitivity to crossing fiber confounds. It is also interesting to note that the posterior limb of the internal capsule on the ViSTA aMWF maps looks particularly brighter, potentially delineating the corticospinal tracts (compare with FA maps).

3.3. Correlation with clinical outcomes

Regarding the relationship between mean global aMWF, FA, and RD values and clinical outcomes in TBI (Table 3), all three global MRI

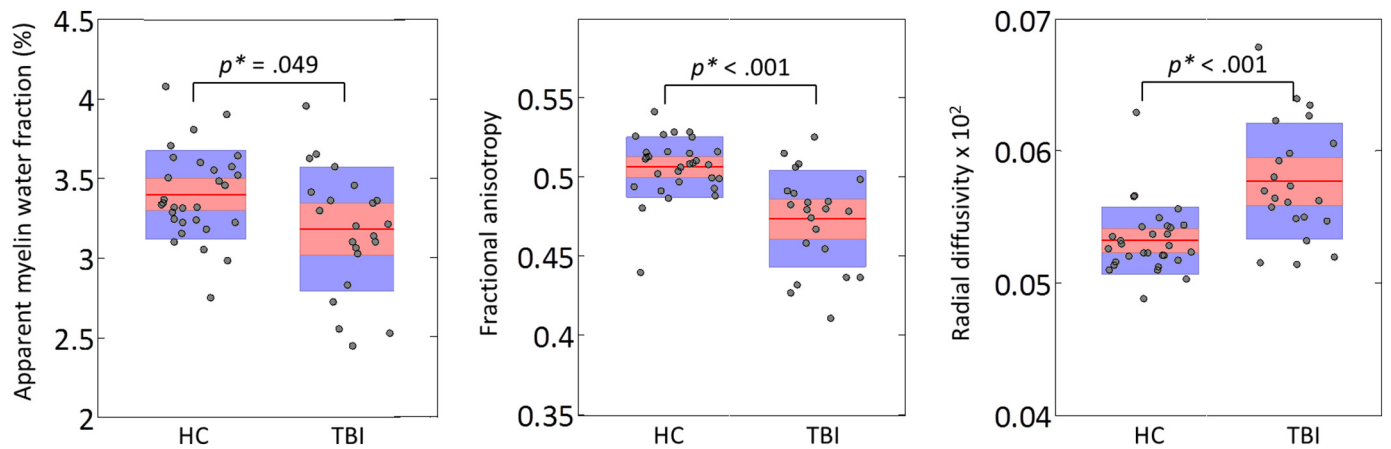


Fig. 2. The mean global aMWF, FA, and RD in HC and TBI patients. Mann-Whitney U test was performed for statistical differences between the groups ($p^* < .05$).

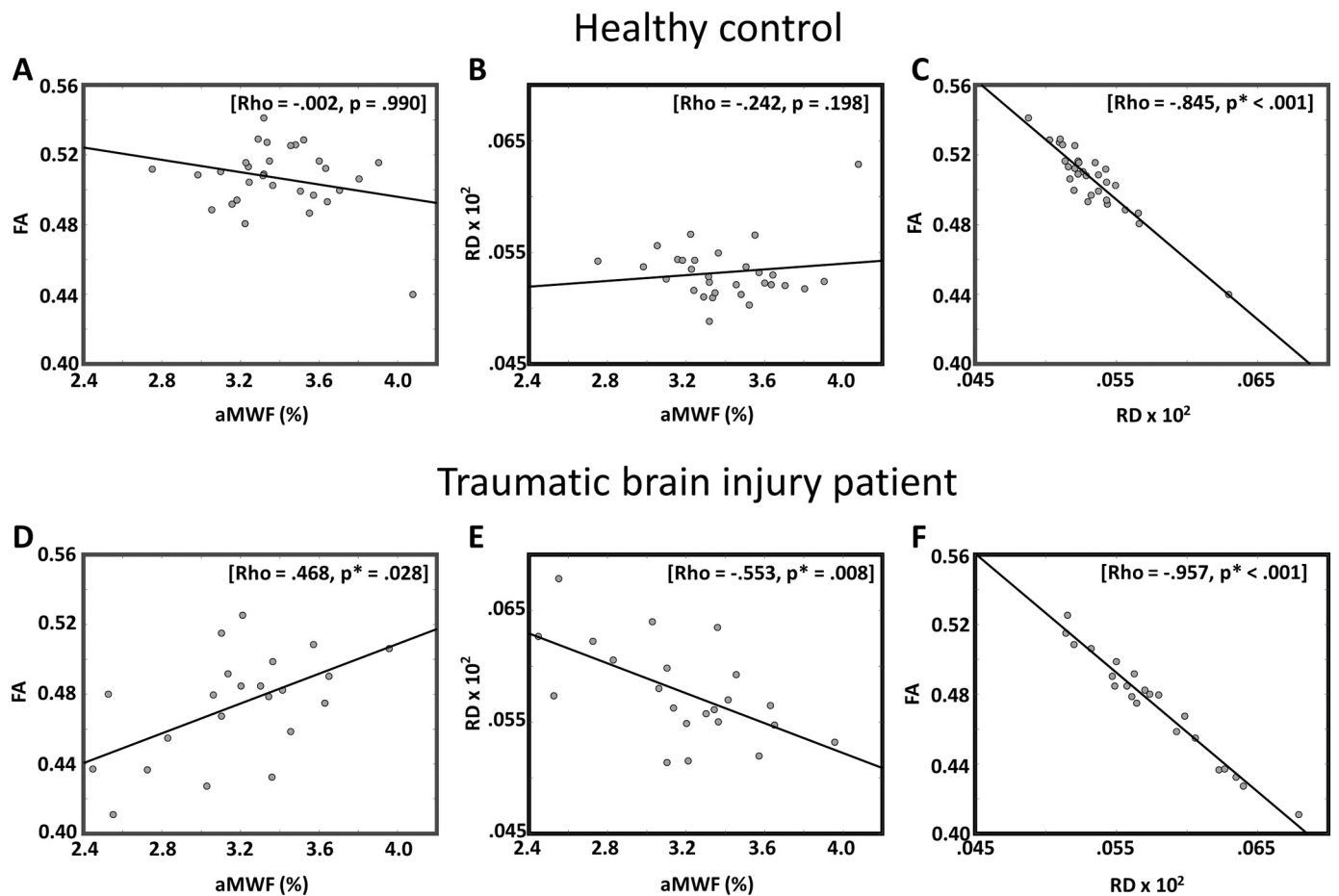


Fig. 3. Scatter plots (A, D) between aMWF and FA, (B, E) between aMWF and RD, and (C, F) between FA and RD. (A), (B), and (C) are in HC whereas (D), (E), and (F) are in TBI. aMWF was not significantly correlated with FA and RD. Rho and p in the brackets denote Spearman's correlation coefficient and p value, respectively. Asterisk shows significance ($p < .05$).

metrics were significantly correlated with PTA (aMWF; $r = -0.564$ and $p = .006$, FA; $r = -0.647$ and $p = .001$, and RD; $r = 0.675$ and $p = .001$). With regard to PSI, only the correlation with aMWF reached statistical significance ($r = 0.452$ and $p = .035$). However, given our small sample size, it should be noted that there was also a clear trend toward significant association with DTI metrics (FA; $r = 0.405$ and $p = .062$ and RD; $r = -0.367$ and $p = .092$). Fig. 5 shows the scatter plots between mean global aMWF, FA, and RD values and clinical outcomes (PTA and PSI).

4. Discussion

In the present study, we observed widespread changes in myelin water measured by ViSta MWI in persons with moderate to severe TBI at 3 months post-injury. In a previous MWI study of concussed college hockey players, MWF values were found to recover to a normal level by 2 months post-injury (Wright et al., 2016). In our cohort, however, the more severe injury appeared to lead to a more persistent reduction in myelin water. Our findings are in line with previous studies that

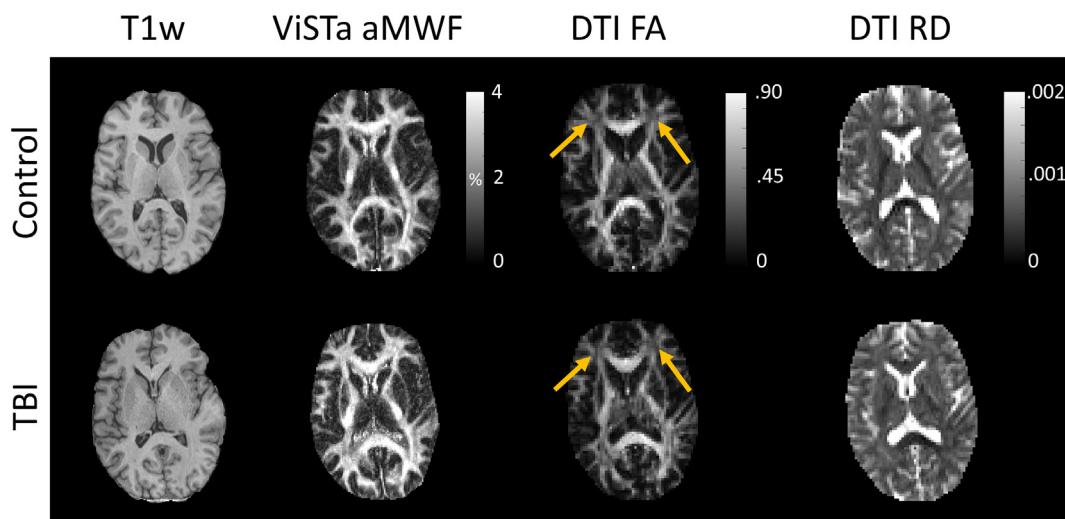


Fig. 4. Representative T₁ weighted (first column), ViSta aMWF (second column), FA (third column), and RD (fourth column) images in a HC (upper row) and a patient with diffuse TBI in the absence of focal lesion (lower row). Arrows point to areas with crossing fibers.

Table 3
Spearman's correlation coefficient between MR metrics (aMWF, FA, and RD) and clinical outcomes (PSI and PTA) in TBI.

	aMWF	FA	RD
PSI	0.452 (0.035)*	0.405 (0.062)	-0.367 (0.092)
PTA	-0.564 (0.006)*	-0.647 (0.001)**	0.675 (0.001)**

The numbers in the parentheses are *p* values. aMWF: apparent myelin water fraction, FA: fractional anisotropy, RD: radial diffusivity, PSI: processing speed index, and PTA: post traumatic amnesia.

* *p* < .05.

** *p* < .01.

speculated the injury to central myelin may contribute to axonal degeneration following TBI over a period of months to several years (Maxwell, 2013).

We also found that reduced aMWF was proportional to the severity of TAI as estimated by the duration of PTA. This finding supports the notion that MWI may serve as a biomarker to assess the extent of axonal and myelin damage in patients with TAI. We also found that aMWF was significantly correlated with PSI, which suggests that myelin injury may be particularly relevant to processing speed deficits after TBI. PSI is known as a sensitive behavioral index of the overall extent of diffuse brain injury and is a clinically important phenomenon related to attention, memory, and communication abilities (Kennedy et al., 2003). Recent studies have demonstrated that myelinated fibers play a central role in brain messaging and supports processing speed (Chevalier et al., 2015). Additionally, studies have reported that myelin thickness is also positively related to signal conduction velocity in the brain (Waxman, 1980). Taken together with previous findings, this study strongly suggests that impairment in neural signaling due to moderate to severe brain injury is significantly related to decreases in myelin water.

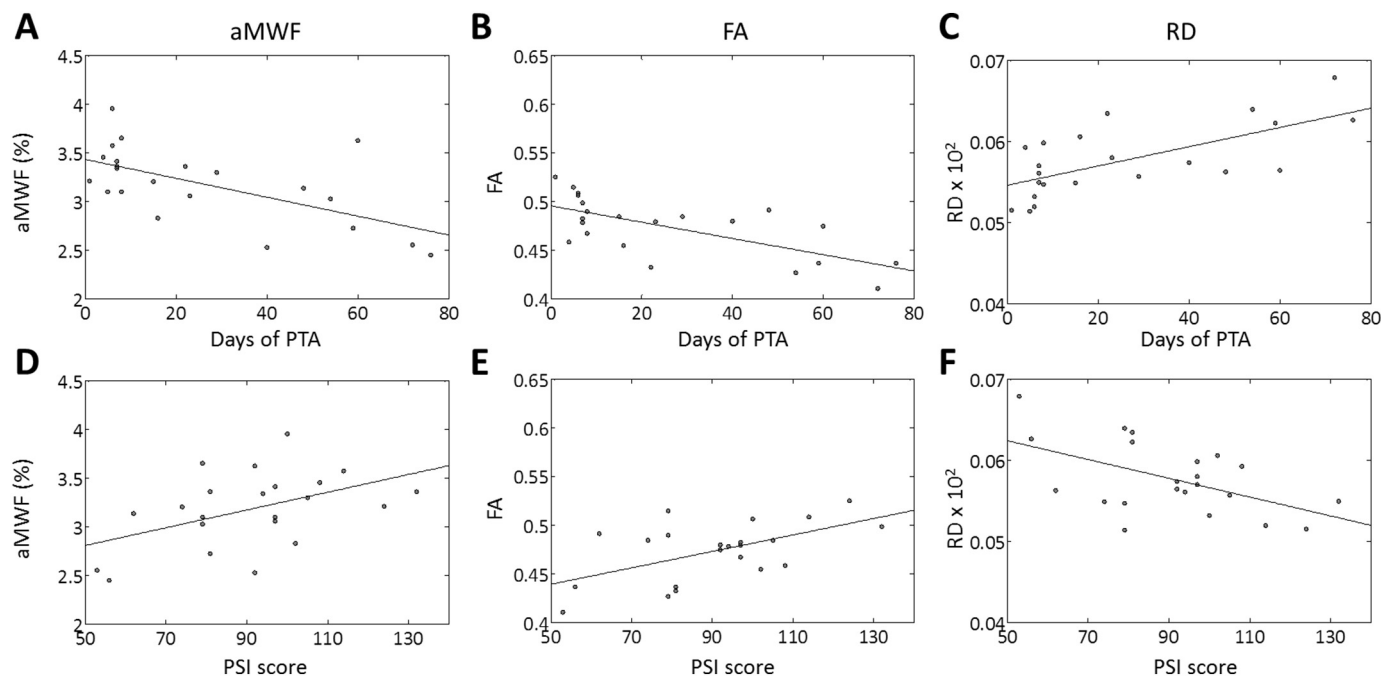


Fig. 5. Scatter plots between days of post-traumatic brain injury (PTA) and aMWF (A), FA (B), and RD (C), and between processing speed index (PSI) scores and aMWF (D), FA (E), and RD (F).

The relationship among different MRI metrics revealed an interesting pattern. Many researchers have hypothesized that RD indirectly represents the amount of demyelination. In line with this notion are our findings that RD showed higher correlations with aMWF than FA. However, we also found that the correlation between RD and aMWF was only moderate. The fact that aMWF and DTI metrics are only moderately correlated to each other suggests that aMWF may potentially provide complementary information to conventional DTI. As mentioned in the introduction, DTI parameters are affected by various components such as the neurofibrils, axonal membrane, myelin sheath, and intra- and extra-cellular structure in WM (Beaulieu, 2002). Since TBI causes increased inter-axonal water where axons and myelin are lost (Wozniak et al., 2007), FA and RD may reflect mixed and accumulated signal changes. Recent evidence suggests that DTI metrics may not be specific to myelin integrity (Chiang et al., 2014; Wang et al., 2014). The present study employed ViSta MWI, which is a method that indirectly detects the extent of myelin damage in TBI with high image quality. Although the acquisition method between ViSta MWI and conventional MWI is different, many studies have supported that ViSta aMWF originates from myelin water (Kim et al., 2015; Lee et al., 2014; Oh et al., 2013; Oh et al., 2014). Therefore, it is reasonable to conclude that reductions in ViSta aMWF in our participants with TBI reflect myelin damage due to brain injury.

This study has several limitations that bear noting. First, direct voxel-based comparison of aMWF and DTI metrics could not be done in this study due to the challenge of registering two modalities into a common space. A future study that acquires aMWF and DTI metrics with the same resolution would allow voxel-based comparison between different modalities with minimum registration error. Second, the correlational analysis was based on data from 22 TBI patients. In this small sample, null findings (i.e. lack of significant correlation between PSI and DTI measures) may be due to inadequate power, and hence, should be interpreted with caution. Third, the meaning of moderate correlation between aMWF and DTI metrics needs to be carefully interpreted. It may reflect either the fact that the metrics measure complementary phenomena or that there is measurement error due to low reproducibility. Despite that our previous preliminary work has shown that aMWF has very high voxel-wise reproducibility ($r = 0.97$) (Oh et al., 2014), any biophysical interpretation requires caution. Fourth, the global values were mainly used in this study. To address this concern, we further analyzed group difference between HC and TBI using aMWF in the corpus callosum, as shown in supplementary Fig. 2. The statistical significance was comparable with that based on the global aMWF values. We suspect that small regions of interest might be more vulnerable to random noise. Fifth, related to previous point, histological studies would eventually be needed to clearly elucidate the pathophysiologicals contributing to aMWF, FA, and RD. Finally, we examined persons with TBI at 3 months following injury. It would be of interest to study the clinical correlates, if any, of the imaging measures used in this study at a later point in the recovery process.

5. Conclusions

For the first time, this study compared aMWF in moderate to severe TBI patients at 3 months post-injury to that in HC. Current results demonstrated reduced aMWF is prevalent in moderate to severe diffuse TBI patients. This implies that TBI causes demyelination of the white matter. Additionally, aMWF was significantly correlated with measures of injury severity and neurocognitive performance. We believe that aMWF could serve as a potential biomarker for injury severity of myelin and prediction of clinical outcomes.

Funding sources

This work was supported in part by the NIH (NINDS) grant 5R01NS065980, by Creative-Pioneering Researchers Program through

Seoul National University (SNU), by the Brain Research Program through the National Research Foundation of Korea (NRF) funded by the Ministry of Science, ICT & Future Planning (2017R1A2B2008412).

Conflict of interest

No conflict of interest or industry support.

Appendix A. Supplementary data

Supplementary data to this article can be found online at <https://doi.org/10.1016/j.nicl.2019.101785>.

References

- Avants, B., Gee, J.C., 2004. Geodesic estimation for large deformation anatomical shape averaging and interpolation. *Neuroimage* 23 (Suppl. 1), S139–S150.
- Avants, B.B., Yushkevich, P., Pluta, J., Minkoff, D., Korczykowski, M., Detre, J., Gee, J.C., 2010. The optimal template effect in hippocampus studies of diseased populations. *Neuroimage* 49, 2457–2466.
- Beaulieu, C., 2002. The basis of anisotropic water diffusion in the nervous system - a technical review. *NMR Biomed.* 15, 435–455.
- Bramlett, H.M., Dietrich, W.D., 2002. Quantitative structural changes in white and gray matter 1 year following traumatic brain injury in rats. *Acta Neuropathol.* 103, 607–614.
- Chevalier, N., Kurth, S., Doucette, M.R., Wiseheart, M., Deoni, S.C., Dean 3rd, D.C., O'Muircheartaigh, J., Blackwell, K.A., Munakata, Y., LeBourgeois, M.K., 2015. Myelination is associated with processing speed in early childhood: preliminary insights. *PLoS One* 10, e0139897.
- Chiang, C.W., Wang, Y., Sun, P., Lin, T.H., Trinkaus, K., Cross, A.H., Song, S.K., 2014. Quantifying white matter tract diffusion parameters in the presence of increased extra-fiber cellularity and vasogenic edema. *Neuroimage* 101, 310–319.
- Choi, J.Y., Jeong, I.H., Oh, S.H., Oh, C.H., Kim, H.J., Lee, J., 2016. A quantitative evaluation of normal appearing white matter in multiple sclerosis: ViSta MWI and SE MWI. *Proc Intl Soc Mag Reson Med* 25th.
- Choi, J.Y., Jeong, I.H., Oh, S.H., Oh, C.H., Park, N.Y., Kim, H.J., Lee, J., 2018. Evaluation of normal-appearing white matter in multiple sclerosis using direct visualization of short transverse relaxation time component (ViSta) myelin water imaging and Gradient Echo and Spin Echo (GRASE) myelin water imaging. *J. Magn. Reson. Imaging* 49, 1091–1098.
- Felmingham, K.L., Baguley, J.J., Green, A.M., 2004. Effects of diffuse axonal injury on speed of information processing following severe traumatic brain injury. *Neuropsychology* 18, 564–571.
- Jackson, W.T., Novack, T.A., Dowler, R.N., 1998. Effective serial measurement of cognitive orientation in rehabilitation: the Orientation Log. *Arch. Phys. Med. Rehabil.* 79, 718–720.
- Jeong, I.H., Choi, J.Y., Kim, S.H., Hyun, J.W., Joung, A., Lee, J., Kim, H.J., 2017. Normal appearing white matter demyelination in neuromyelitis optica spectrum disorder. *Eur. J. Neurol.* 24, 652–658.
- Jurick, S.M., Bangen, K.J., Evangelista, N.D., Sanderson-Cimino, M., Delano-Wood, L., Jak, A.J., 2016. Advanced neuroimaging to quantify myelin in vivo: application to mild TBI. *Brain Inj.* 30, 1452–1457.
- Katz, D.I., Alexander, M.P., 1994. Traumatic brain injury. Predicting course of recovery and outcome for patients admitted to rehabilitation. *Arch. Neurol.* 51, 661–670.
- Kennedy, J.E., Clement, P.F., Curtiss, G., 2003. WAIS-III processing speed index scores after TBI: the influence of working memory, psychomotor speed and perceptual processing. *Clin. Neuropsychol.* 17, 303–307.
- Kim, D., Lee, H.M., Oh, S.H., Lee, J., 2015. Probing signal phase in direct visualization of short transverse relaxation time component (ViSta). *Magn. Reson. Med.* 74, 499–505.
- Kinnunen, K.M., Greenwood, R., Powell, J.H., Leech, R., Hawkins, P.C., Bonnelle, V., Patel, M.C., Counsell, S.J., Sharp, D.J., 2011. White matter damage and cognitive impairment after traumatic brain injury. *Brain* 134, 449–463.
- Kraus, M.F., Susmaras, T., Caughlin, B.P., Walker, C.J., Sweeney, J.A., Little, D.M., 2007. White matter integrity and cognition in chronic traumatic brain injury: a diffusion tensor imaging study. *Brain* 130, 2508–2519.
- Landman, B.A., Wan, H., Bogovic, J.A., Bazin, P.L., Prince, J.L., 2010. Resolution of crossing fibers with constrained compressed sensing using traditional diffusion tensor MRI. *Proc. SPIE Int. Soc. Opt. Eng.* 7623, 76231h.
- Lee, H.M., Kim, D., Oh, S.S., Choi, J.Y., Oh, S.H., Lee, J., 2014. The phase and magnetization transfer characteristics of a novel myelin water imaging method (ViSta). *Proc Intl Soc Mag Reson Med #0338*, May 10–16, Milan, Italy.
- Liu, C., Li, W., Johnson, G.A., Wu, B., 2011. High-field (9.4 T) MRI of brain dysmyelination by quantitative mapping of magnetic susceptibility. *Neuroimage* 56, 930–938.
- Maas, A.L., Stocchetti, N., Bullock, R., 2008. Moderate and severe traumatic brain injury in adults. *Lancet Neurol.* 7, 728–741.
- Mathias, J.L., Wheaton, P., 2007. Changes in attention and information-processing speed following severe traumatic brain injury: a meta-analytic review. *Neuropsychology* 21, 212–223.
- Maxwell, W.L., 2013. Damage to myelin and oligodendrocytes: a role in chronic outcomes following traumatic brain injury? *Brain Sci* 3, 1374–1394.

- Mierzwa, A.J., Marion, C.M., Sullivan, G.M., McDaniel, D.P., Armstrong, R.C., 2015. Components of myelin damage and repair in the progression of white matter pathology after mild traumatic brain injury. *J. Neuropathol. Exp. Neurol.* 74, 218–232.
- Newcombe, V.F., Williams, G.B., Nortje, J., Bradley, P.G., Harding, S.G., Smielewski, P., Coles, J.P., Maiya, B., Gillard, J.H., Hutchinson, P.J., Pickard, J.D., Carpenter, T.A., Menon, D.K., 2007. Analysis of acute traumatic axonal injury using diffusion tensor imaging. *Br. J. Neurosurg.* 21, 340–348.
- Ng, H.K., Mahaliyana, R.D., Poon, W.S., 1994. The pathological spectrum of diffuse axonal injury in blunt head trauma: assessment with axon and myelin strains. *Clin. Neurol. Neurosurg.* 96, 24–31.
- Oh, S.H., Bilello, M., Schindler, M., Markowitz, C.E., Detre, J.A., Lee, J., 2013. Direct visualization of short transverse relaxation time component (ViSta). *Neuroimage* 83, 485–492.
- Oh, S.H., Choi, J.Y., Im, Y., Prasloski, T., Lee, J., 2014. Myelin water fraction of the whole brain: 3D grase MWI vs 3D ViSta MWI. *Proc Intl Soc Mag Reson Med #3143*, May 10–16, Milan, Italy.
- Ponsford, J., 2013. Factors contributing to outcome following traumatic brain injury. *NeuroRehabilitation* 32, 803–815.
- Ross, B.L., Temkin, N.R., Newell, D., Dikmen, S.S., 1994. Neuropsychological outcome in relation to head injury severity. Contributions of coma length and focal abnormalities. *Am J Phys Med Rehabil* 73, 341–347.
- Sharp, D.J., Beckmann, C.F., Greenwood, R., Kinnunen, K.M., Bonnelle, V., De Boissezon, X., Powell, J.H., Counsell, S.J., Patel, M.C., Leech, R., 2011. Default mode network functional and structural connectivity after traumatic brain injury. *Brain* 134, 2233–2247.
- Shenton, M.E., Hamoda, H.M., Schneiderman, J.S., Bouix, S., Pasternak, O., Rathi, Y., Vu, M.A., Purohit, M.P., Helmer, K., Koerte, I., Lin, A.P., Westin, C.F., Kikinis, R., Kubicki, M., Stern, R.A., Zafonte, R., 2012. A review of magnetic resonance imaging and diffusion tensor imaging findings in mild traumatic brain injury. *Brain Imaging Behav* 6, 137–192.
- Smith, S.M., 2002. Fast robust automated brain extraction. *Hum. Brain Mapp.* 17, 143–155.
- Smith, S.M., Nichols, T.E., 2009. Threshold-free cluster enhancement: addressing problems of smoothing, threshold dependence and localisation in cluster inference. *Neuroimage* 44, 83–98.
- Smith, S.M., Jenkinson, M., Johansen-Berg, H., Rueckert, D., Nichols, T.E., Mackay, C.E., Watkins, K.E., Ciccarelli, O., Cader, M.Z., Matthews, P.M., Behrens, T.E., 2006. Tract-based spatial statistics: voxelwise analysis of multi-subject diffusion data. *Neuroimage* 31, 1487–1505.
- Wang, X., Cusick, M.F., Wang, Y., Sun, P., Libbey, J.E., Trinkaus, K., Fujinami, R.S., Song, S.K., 2014. Diffusion basis spectrum imaging detects and distinguishes coexisting subclinical inflammation, demyelination and axonal injury in experimental autoimmune encephalomyelitis mice. *NMR Biomed.* 27, 843–852.
- Waxman, S.G., 1980. Determinants of conduction velocity in myelinated nerve fibers. *Muscle Nerve* 3, 141–150.
- Wechsler, D., Coalson, D.S.R., 2008. WAIS-IV: Wechsler adult intelligence scale. Pearson, San Antonio, TX.
- Winkler, A.M., Ridgway, G.R., Webster, M.A., Smith, S.M., Nichols, T.E., 2014. Permutation inference for the general linear model. *Neuroimage* 92, 381–397.
- Wozniak, J.R., Krach, L., Ward, E., Mueller, B.A., Muetzel, R., Schnoebelen, S., Kiragu, A., Lim, K.O., 2007. Neurocognitive and neuroimaging correlates of pediatric traumatic brain injury: a diffusion tensor imaging (DTI) study. *Arch. Clin. Neuropsychol.* 22, 555–568.
- Wright, A.D., Jarrett, M., Vavasour, I., Shahinfard, E., Kolind, S., van Donkelaar, P., Taunton, J., Li, D., Rauscher, A., 2016. Myelin water fraction is transiently reduced after a single mild traumatic brain injury—a prospective cohort study in collegiate hockey players. *PLoS One* 11, e0150215.